Int. J. Cancer: **104,** 782–789 (2003)

Publication of the International Union Against Cancer

PHOTODYNAMIC THERAPY WITH Pd-BACTERIOPHEOPHORBIDE (TOOKAD): SUCCESSFUL *IN VIVO* TREATMENT OF HUMAN PROSTATIC SMALL CELL CARCINOMA XENOGRAFTS

Natalia V. KOUDINOVA[1], Jehonathan H. PINTHUS[2,6], Alexander BRANDIS[3], Ori BRENNER[4], Peter BENDEL[5], Jacob RAMON[6], Zelig ESHHAR[2], Avigdor SCHERZ[3] and Yoram SALOMON[1]*

[1]*Department of Biological Regulation, The Weizmann Institute of Science, Rehovot, Israel*
[2]*Department of Immunology, The Weizmann Institute of Science, Rehovot, Israel*
[3]*Department of Plant Science, The Weizmann Institute of Science, Rehovot, Israel*
[4]*Experimental Animal Center, The Weizmann Institute of Science, Rehovot, Israel*
[5]*Department of Chemical Services, The Weizmann Institute of Science, Rehovot, Israel*
[6]*Department of Urology, Sheba Medical Center, Tel Hashomer, Israel*

Small cell carcinoma of the prostate (SCCP), although relatively rare, is the most aggressive variant of prostate cancer, currently with no successful treatment. It was therefore tempting to evaluate the response of this violent malignancy and its bone lesions to Pd-Bacteriopheophorbide (TOOKAD)-based photodynamic therapy (PDT), already proven by us to efficiently eradicate other aggressive non-epithelial solid tumors. TOOKAD is a novel bacteriochlorophyll-derived, second-generation photosensitizer recently, developed by us for the treatment of bulky tumors. This photosensitizer is endowed with strong light absorbance ($\epsilon_0 \sim 10^5$ mol^{-1} cm^{-1}) in the near infrared region (λ=763nm), allowing deep tissue penetration. The TOOKAD-PDT protocol targets the tumor vasculature leading to inflammation, hypoxia, necrosis and tumor eradication. The sensitizer clears rapidly from the circulation within a few hours and does not accumulate in tissues, which is compatible with the treatment of localized tumor and isolated metastases. Briefly, male CD1-nude mice were grafted with the human SCCP (WISH-PC2) in 3 relevant anatomic locations: subcutaneous (representing tumor mass), intraosseous (representing bone metastases) and orthotopically within the murine prostate microenvironment. The PDT protocol consisted of i.v. administration of TOOKAD (4 mg/kg), followed by immediate illumination (650–800 nm) from a xenon light source or a diode laser emitting at 770 nm. Controls included untreated animals or animals treated with light or TOOKAD alone. Tumor volume, human plasma chromogranin A levels, animal well being and survival were used as end points. In addition, histopathology and immunohistochemistry were used to define the tumor response. Subcutaneous tumors exhibited complete healing within 28–40 days, reaching an overall long-term cure rate of 69%, followed for 90 days after PDT. Intratibial WISH-PC2 lesions responded with complete tumor elimination in 50% of the treated mice at 70–90 days after PDT as documented histologically. The response of the orthotopic model was also analyzed histologically with similar results. The study with this model suggests that TOOKAD-based PDT can reach large tumors and is a feasible, efficient and well-tolerated approach for minimally invasive treatment of local and disseminated SCCP.

Key words: *photodynamic therapy; small cells carcinoma of prostate; bone metastasis; palladium-Bacteriopheophorbide; xenograft*

Prostate cancer (PC) is the most commonly diagnosed noncutaneous malignancy and is the second leading cause of cancer death among American males. Moreover, PC is the cause of substantial morbidity and serious complications from local growth and distant metastases that affect the quality of life of many patients. To successfully combat primary, advanced and metastatic PC, new therapeutic strategies are required.

Photodynamic therapy (PDT) is a mode of cancer therapy in which drug action is locally controlled by light. In PDT, *in-situ* photosensitization of a non-toxic sensitizer generates cytotoxic reactive oxygen species (ROS) that cause cell death and necrosis of tumor components, with minimal damage to the surrounding tissue.[1–4] In general, treatment selectivity of PDT results from differential drug accumulation within the tumor and normal tissue combined with site-specific illumination that, by use of an optic fiber, can reach tumors in practically any organ. PDT has been clinically applied to superficial tumors directly accessible to illumination, such as cutaneous basal cell carcinoma,[5] head and neck tumors,[6] esophageal carcinoma[7] and lung carcinoma.[8,9] In urology PDT has been mainly applied for the treatment of transitional cell carcinoma of the bladder,[10–13] but it has not yet been considered applicable for PC treatment. Several investigators reported on experiments with PDT of normal prostate and PC. However, these reports were mainly concerned with light transmission through prostatic tissue[14–18] and PC.[19] Studies concerning PDT of the normal canine prostate[20] and of subcutaneous or orthotopic rat Dunning R3327 tumors[21–23] have been reported. To the best of our knowledge, there is presently no published clinical PDT protocol for human prostate cancer except for one report (letter to the editor) that had no follow-up.[24] The clinical application of PDT as a treatment option for primary, locally advanced and certainly for disseminated PC could not be realized thus far, primarily because of spectral properties of available sensitizers that limit the depth of treatment and hence the tumor mass affected.[3,25] In addition the sensitizers used so far significantly accumulated in the skin subjecting patients to prolonged cutaneous phototoxicity.[25]

Bachteriochlorophyll derivatives synthesized in our laboratory,[26–30] in collaboration with Steba Biotech NV., The Netherlands,

Abbreviations: hCgA, human chromogranin A; HNE, 4-hydroxy-2-nonenal; LPO, lipid peroxidation, MRI, magnetic resonance imaging; PC, prostate cancer; PDT, photodynamic therapy; ROS, reactive oxygen species; SCCP, small cell carcinoma of the prostate; WISH-PC2, Weizmann Sheba prostate cancer 2.

Grant sponsor: CaP CURE, and STEBA BIOTECH, NV., The Netherlands.

Natalia V. Koudinova and Jehonathan H. Pinthus contributed equally to this article.

*Correspondence to: The Department of Biological Regulation, The Weizmann Institute of Science, Rehovot, 76100, Israel
Tel/fax: 972-8-934-3930/4116, E-mail: yoram.salomon@weizmann.ac.il

Received 11 July 2002; Revised 29 October 2002, 5 December 2002; Accepted 6 December 2002

DOI 10.1002/ijc.11002

and Negma LeRads, France, have several advantages that overcome the above limitations and enable treatment of larger tumor masses. They include Bacteriochlorophyll-Serine[31,32] and in particular Pd-bacteriopheophorbide (TOOKAD)[28,33] (Scherz A, 2002, personal communications), which was shown to induce lesions of over 3 cm in diameter in the dog prostate and was recently suggested as an alternative modality for prostate cancer therapy.[23] TOOKAD has a major absorption band at 763 nm and rapidly clears from the circulation (95% within 10 min).[34] From most other tissues it clears within a number of hours, with transient accumulation in the liver, from which it completely clears within 48 hr (Scherz A, 2002, personal communications).[34] In contrast to clinically used photosensitizers, the therapeutic action of TOOKAD, much like its predecessor Bacteriochlorophyll-serine,[31] is by destruction of the tumor vasculature and not by direct tumor cell kill (Scherz A, 2002, personal communications).[33]

We have previously shown that illumination of rat C6 glioma xenografts shortly after i.v. injection of TOOKAD induces tumor vascular damage that leads to vessel constriction, hypoxia and tumor eradication.[33,35] Using the same PDT protocol with Bacteriochlorophyll-serine for treatment of melanoma[31] and DS sarcoma,[32] we obtained similar results. The effectiveness of TOOKAD-based PDT in destroying prostatic tissue in a canine prostate model, with no evidence of urinary side effects,[23] and lack of skin toxicity in the rat (Koudinova et al., 2002, unpublished) have recently been demonstrated. TOOKAD may therefore overcome the main drawbacks of clinically used sensitizers, including the problem of prolonged cutaneous phototoxicity presently encountered with clinically used sensitizers, and broaden the scope of the PDT modality for prostate cancer therapy.

Primary and local, recurrent prostate tumors are amenable to PDT due to their accessible anatomical location. Consequently, simultaneous direct real-time visualization by transrectal ultrasonography combined with interstitial fiber optic illumination via trans-perineal route is feasible.[36] In addition, this modality can provide palliation for isolated, accessible metastatic lesions. To prove this concept, we elected to initially examine the response to TOOKAD-PDT of the most aggressive form of human prostate cancer, SCCP and its metastatic bone lesions in immunodeficient nude mice. The model used in our study, WISH-PC2, was recently described by us.[37]

In the present study, we demonstrate, for the first time, a substantial curative response of a relatively large tumor mass of human prostate xenografts, as well as established bone lesions, using a single treatment regimen of TOOKAD-PDT. The results obtained suggest that TOOKAD-PDT is a feasible, efficient and well-tolerated approach for noninvasive and mini-invasive treatment of local and disseminated SCCP.

MATERIAL AND METHODS

Photosensitizer

Pd-bacteriopheophorbide (TOOKAD, Steba-Biotech NV., The Netherlands) (10 mg) was dissolved in a Cremophor EL-based vehicle (Sigma Diagnostic, St. Louis, MO), as described earlier (Scherz A, 2002, personal communications). The sensitizer concentration was determined spectroscopically at 763 nm, assuming ($\epsilon_0 = 10.86\times10^4$ mol^{-1} cm^{-1}) upon dilution in chloroform.

Animals

Male CD1 nude mice (28–32 g) were housed and handled in the animal facility according to the guidelines (1996) of the Weizmann Institute of Science, Rehovot, Israel.

Xenograft model

Single-cell suspensions of WISH-PC2[37] were mixed with Matrigel (Becton Dickinson, Bedford, MA) (1:1, v/v) and implanted into the mice: subcutaneously (s.c.) ($10–15\times10^6$ cells/mouse), intraosseous (i.o.) into proximal tibia (2×10^6 cells/mouse) and orthotopic into the dorsal prostatic lobe through the midline, lower abdominal incision (2×10^6 cells/mouse).[38] Tumors of the s.c. model reached treatment size, diameter of 7–9 mm within 3–4 weeks. Intraosseous xenografts were identified and localized by MRI within 4–5 weeks. Orthotopic implants were identified by palpation and reached treatment size (5–7 mm) within 3–5 weeks after implantation.

Anesthesia

Animals were i.p. injected with a mixture of 5 mg/kg ketamine (Rhone Merieux, Lyon, France) and 1 mg/kg rompun (Bayer, Leverkusen, Germany) (85:15, v:v).

Light sources

The light sources were as follows: light source, #1, Xenon fluoride lamp (Biospec, Russia) equipped with a 650–800 nm spectral window and optic fibers, and light source #2, a 150 mW fiber-equipped diode laser emitting light at 770 nm (Biospec, Russia). Light source #2 was used either with a 0.6 cm diffuser for interstitial illumination or with a flat-cut fiber for transcutaneous illumination as described.

PDT protocol

Anesthetized mice were i.v. injected (tail vein) with TOOKAD (4 mg/kg) and subcutaneous tumor or intraosseous xenografts were immediately illuminated transcutaneously for 30 min with light source number 1 at a dose of 360 J/cm,^{2} using a light field of 14–16 mm diameter. Orthotopic xenografts were exposed *via* a midline abdominal incision and the optic fiber was implanted into the tumor perpendicular to the abdominal wall. Illumination was interstitially delivered at a dose of 54 J/0.6 cm (30 mW/0.6 cm/30 min) with light source #2. After treatment, the animals were returned to the cage. Tumor response was recorded photographically and histologically, and i.o. tumors were also recorded by MRI. The volume (mm^3) of s.c. tumors was determined by caliper measurement using the formula: length $\times$ width $\times$ depth $\times$ 0.5236.[39] The controls were the following: dark control, the mice were i.v. injected with sensitizer and placed in a dark cage (24 hr) without illumination, and light control, tumors in uninjected mice were illuminated under standard conditions. Animal survival (s.c. and i.o. models) was followed for up to 70–90 days after PDT. In accordance with the Weizmann Institute Animal's ethics committee guidelines, the animals were euthanized to avoid tumor burden when their tumor volume approached $\sim$ 2,000 mm.^{3} All therapeutic results relate to only one treatment session.

MRI examination

MRI was performed using a 4.7 T spectrometer with a horizontal magnet (Bruker-"Biospec," Germany). The anesthetized mice were placed with their legs positioned above the center of the surface coil. The anatomy and morphology of the tibia were examined on both axial (perpendicular to the bone axis) and coronal (parallel to the bone axis) MRI slices. The MRI was based on a T2-weighted fast spin echo (FSE) protocol, typically with the following acquisition parameters: 256$\times$256 matrix, 8 echoes per excitation with an effective TE of 67 ms, TR of 3,720 ms, slice thickness of 2 mm and field of view of 5 cm, with 2 averages.

Histology

The mice were sacrificed and the tumors excised and placed in buffered (phosphate buffer: 25 mM NaH_2PO_4, 45 mM Na_2HPO_4, pH=7.4) 4% formaldehyde medium at room temperature for 24 hr. The tumors were then processed and stained with hematoxyline/eosin under standard conditions. Light microscopy was performed with a microscope (Nikon Optiphot 2, Japan) equipped with a digital camera (DVC Company, Inc., Austin, TX).

Immunohistochemistry

Histological sections were stained for the presence of lipid peroxidation (LPO) products that accumulated in PDT-treated tumors. Paraffin-embedded sections were deparaffinized in xylene and rehydrated by serial incubations in 100%, 95%, and 70%

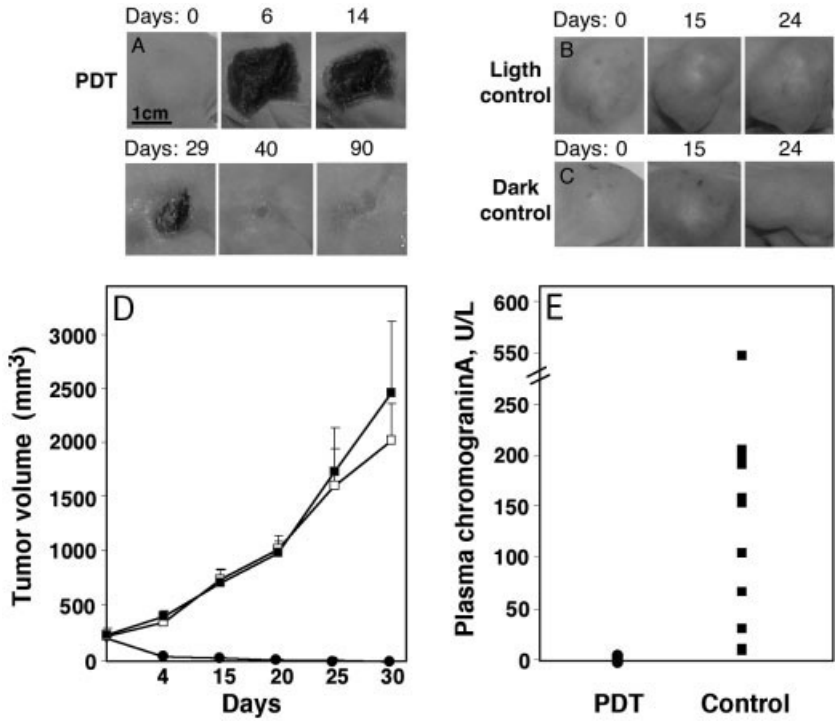

FIGURE 1 – TOOKAD-based PDT of s.c. human WISH-PC2. A typical example of 3 mice representing PDT and control groups is given: (*a*) PDT-induced necrosis is observed within 24–48 hr sustained for 14–29 days, followed by healing (with a complete cure and minimal local scarring) with no recurrence up to 90 days following treatment. (*b*) Light and (*c*) dark controls, the tumors continued to grow and the animals were euthanized by day 24, to avoid tumor burden. (*d*) The tumor volume after PDT was recorded and calculated as described in the Material and Methods. Following PDT (full circles, $n=39$) tumor volume decreased with time, whereas the tumors of the light (full squares, $n=10$) and dark (open squares, $n=10$) control groups continued to grow. Error bars represent ±SD. In total, 27/39 mice of the PDT group survived after 90 days with no evidence of tumor growth. Nine animals exhibited local regrowth at various times (>30 days). To avoid tumor burden, animals were euthanized when tumor volumes reached ~ 2,000 mm^3. (*e*) The individual differences in plasma chromogranin A levels on day of treatment and 21 days post PDT (median = −1 U/L, $n=11$) and control groups (median = 131 U/L, $n=12$) are presented.

ethanol. For early inactivation of endogenous peroxidase, the sections were incubated in 3% H_2O_2 (Merck, Germany), followed by blocking with 1% bovine serum albumin (Sigma Chemical Co., St. Louis, MO) and 2% goat serum in phosphate-buffered saline (PBS). The LPO product 4-hydroxy-2-nonenal (HNE) was identified by incubation with primary rabbit anti-4-hydroxy-2-nonenal HNE antibodies (1:500, Calbiochem, San Diego, CA) for 18 hr at 4°C.[40] After washing with PBS at room temperature (3 times × 20 min), the bound antibody was detected by incubation with secondary goat anti-rabbit Immunoglobulin G antibodies (1:50) coupled to horse radish peroxidase (HRP) and was developed with 3-amino-9-ethylcarbazole (AEC, Sigma Chemical Co.). Samples were co-stained with 0.1% hematoxylin (Sigma Diagnostic, St. Louis, MO).

Determination of plasma human chromogranin A (hCgA)

Evaluation of WISH-PC2 growth was also determined by hCgA, which is produced by this xenograft.[37] Blood for hCgA assessment was collected in cold Eppendorf tubes and centrifuged for 10 min (14,000 rpm, 4°C) until plasma separation. All plasma samples were immediately frozen and stored at −20°C. Plasma hCgA levels were measured by an enzyme-linked immunoabsorbent assay kit as recommended by the manufacturer (Dako A/S, Glostrup, Denmark). Statistical analysis of the results was performed by applying the Mann-Whitney test for comparing the medians of the treated and control groups.

RESULTS

Response of bulky tumor mass of human WISH-PC2 to PDT

First we examined whether a bulky tumor mass of WISH-PC2 responds to TOOKAD-PDT like other aggressive solid tumors and later defined the optimal treatment protocol. Using no drug/light time interval, we based the selected treatment protocol on optimization of light and drug doses. The effectiveness of the selected treatment protocol was then examined (Fig. 1). Animals with approximately 220–250 mm^3 s.c. tumors were selected at random to receive either 1 treatment course of TOOKAD-PDT, TOOKAD alone (dark control) or illumination alone (light control). TOOKAD-PDT ($n=39$) resulted in a local inflammatory response, developing into necrosis that appeared as a dark crust on the skin by 48 hr, reaching a maximal size by 3–6 days (Fig. 1*a*). This process succeeded by tumor healing, culminating in a complete elimination of the tumors by 14–40 days. The follow-up period was extended to 90 days. Local tumor regrowth was observed in 9/39 animals by 30–45 days after PDT, while 3/39 animals died for unknown reasons during the same period. The overall cure rate of s.c. WISH-PC2 by TOOKAD-based PDT was 69% (27/39). Light ($n=10$) (Fig. 1*b*) and dark ($n=10$) (Fig. 1*c*) control tumors were unaffected and the mice had to be euthanized after 30 days due to the huge tumor mass (> 2,000 mm^3). The summary of this experiment is given in Figure 1*d*. Plasma hCgA levels, serving as a surrogate marker for WISH PC2, were determined on the day of treatment and 21 days after treatment, and individual differences were calculated (Fig. 1*e*). The median difference values of the PDT group ($n = 11$) was −1 U/L and that of the untreated controls (n=12) was 131 U/L. The Mann-Whitney test for comparing medians was employed with a one-sided alternative that revealed $p = 0.00003$, which is highly significant. Note that normal mice do not express hCgA.

The effective depth of treatment delivery in this human xenograft model was determined by applying PDT to a large subcutaneous tumor by transcutaneous illumination with the diode laser beam (light source 2) emitting at a dose of 93 J/cm^2 (108 mW/1.16 cm^2/30 min). The results show effective necrosis to a depth of ~1.3 cm along the direction of the laser beam (Fig. 2*a*).

The earliest histological manifestations of TOOKAD-PDT (at 1 hr) consisted of vascular damage characterized by congestion and destruction of blood vessels and multifocal hemorrhages, whereas the tumor cells remained intact (Fig. 2*b*). At 16 hr (Fig. 2*c*) and 24 hr (Fig. 2*d*), cellular degeneration, necrosis and multifocal hemorrhages developed. At 48 hr, tumor degeneration and necrosis with prominent pyknosis and karyorrhexis were more advanced (Fig. 2*e*). At 10 days, complete necrosis and infiltration of mixed inflammatory cells was evident (Fig. 2*f*) and necrotic tissue was surrounded by newly formed granulation tissue (Fig. 2*g*). Histopathological analysis of the untreated tumor tissue (Fig. 2*h*) and the dark control (Fig. 2*i*) revealed intact tumor cells supplied by intact blood vessels. Tumors of the light control had the same

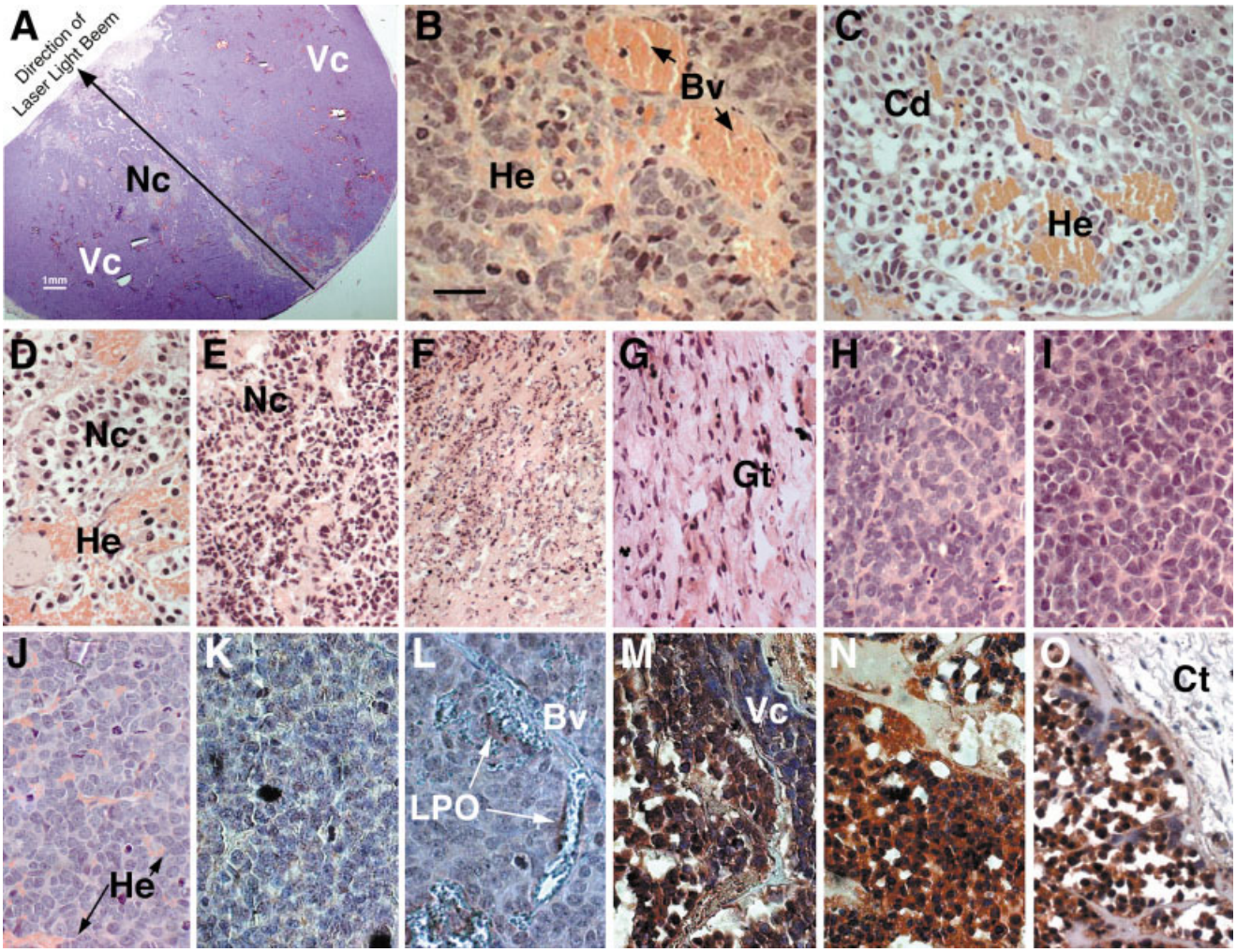

FIGURE 2 – TOOKAD-based PDT of human WISH-PC2: histopathological evaluation. (*a*) The depth of effective PDT in this human WISH-PC2 was assessed on a large s.c. tumor (1,640 mm^2), illuminating transcutaneously with light source #2 at 93 J/cm^2 (108 mW/1.16 cm^2/30 min), demonstrating effective necrosis to a depth of ~1.3 cm along the direction of the laser beam. Necrotic tissue (Nc) is found flanking the line showing the general direction of the laser beam. On both sides of the line a mass of viable tumor cells (Vc) that were not illuminated are seen. By 1 hr after PDT (*b*), congested blood vessels (Bv) and multifocal hemorrhage (He) developed, but tumor cells were still intact. At 16 hr (*c*) and 24 hr (*d*) after PDT, cellular degeneration (Cd) and necrosis (Nc) developed, accompanied by multifocal hemorrhages. At 48 hr after PDT (*e*), large areas of tumor disintegration were observed. Necrotic changes were more advanced with prominent pyknosis and karyorrhexis. Ten days after PDT, the tumor had undergone complete necrosis and liquefaction (*f*) and is surrounded by newly formed granulation tissue (Gt) (*g*). Intact tumor cells are present in the untreated tumor (*h*) and dark control (*i*). In light control (*j*), intact tumor cells accompanied by vascular congestion and scattered hemorrhages. Immunostaining of histological sections exhibited negative HNE staining in untreated tumor (*k*). (*l*) One hour after PDT intensive HNE staining (LPO) is observed around damaged blood vessels. (*m*) Sixteen hours after treatment, positive HNE staining is observed in necrotic regions, whereas the viable cells (Vc) are still negative. By 24 hr (*n*) and 48 hr (*o*) after PDT, the development of necrosis is accompanied by increased positive anti-HNE staining of the tumor and negative staining of connective tissue (Ct). Bar: 20 μm.

architecture, except for occasional scattered hemorrhages (Fig. 2*j*). There was no evidence of tumor necrosis in either control groups.

Consistent with the vascular damage, intensive PDT-induced LPO (observed by anti-HNE-staining) in the blood vessel walls was observed as early as 1 hr after PDT, while weak HNE staining was observed surrounding tumor cells (Fig. 2*l*). At 16 hr, the tumors exhibited PDT-induced necrotic regions coincidental with HNE immunostaining with some yet unaffected tumor cells (Fig. 2*m*). Further development of necrosis and intensification of HNE staining were observed at later times, 24 and 48 hr post-PDT (Fig. 2*n*,*o*, respectively). In contrast, no staining was observed in the surrounding connective tissue (Fig. 2*o*) and in untreated control specimens (Fig. 2*k*). Within 10 days after PDT, no intact cells were observed, and HNE staining was negative (data not shown).

The intraosseous model of WISH-PC2

Tumor response to PDT with TOOKAD (n=22) was also studied using a bone lesion model that was followed for 70–90 days (Fig. 3*a*). The presence and exact location of the tumor implanted into the medullar cavity of the tibia were verified by MRI 4 weeks after implantation, before PDT, in order to accurately deliver the light (Fig.4*a*,*d*). As observed by MRI, tumor growth at the tibial location was totally arrested after PDT with no evident regrowth in the presented mouse, which was monitored at 67 and 90 days post PDT (Figs. 4*b*,*c*). The bright area seen in the tibia after PDT seems to be necrotic bone cortex along with new bone formation, as seen histologically (Fig. 5*a*). Indeed, during this follow-up period, PDT-treated mice had no movement limitations. Tumors of mice in the light (n= 5) and dark (n= 4) control groups grew robustly with the consequent impairment of mobility (Figs. 3*b*,*c*, 4*e*). These

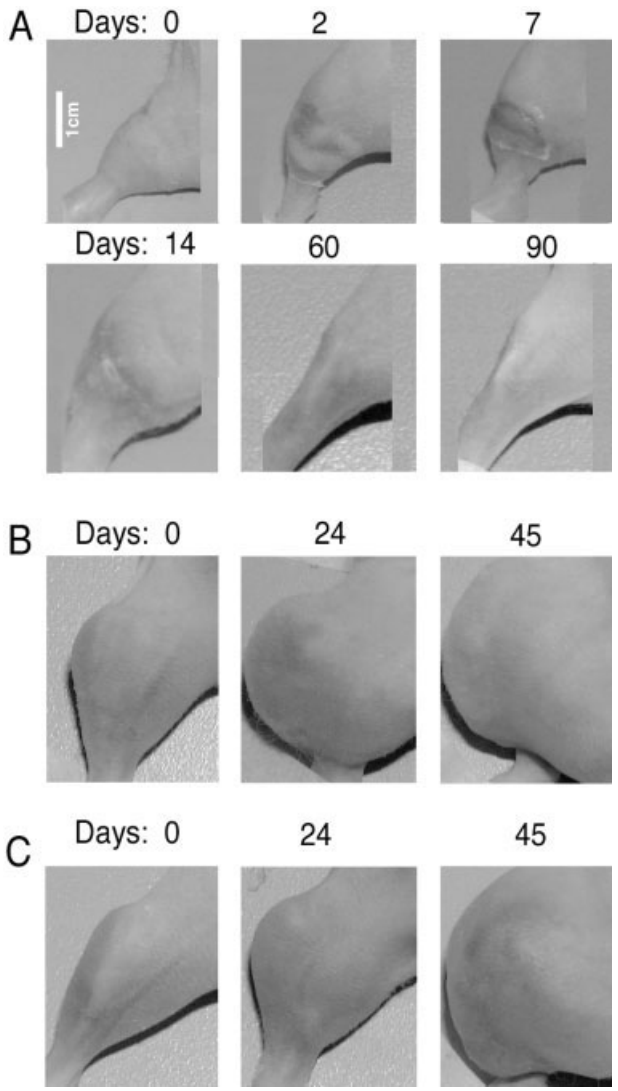

FIGURE 3 – TOOKAD-based PDT of human WISH-PC2 bone lesion model. (*a*) PDT of the tumor by transcutaneous illumination of the leg was followed by visible inflammation on the skin (day 2) and healing by days 7–14, with a complete cure by day 30. The animal was followed up to 90 days after treatment with no evidence of movement difficulties. (*b*,*c*) Light and dark control, respectively. The tumors did not respond to treatment and continued to grow. The animals were sacrificed by day 45 to avoid tumor burden.

animals were sacrificed 50–67 days after treatment to avoid tumor burden. The effect of PDT on bone lesions *per se* was evaluated by histology. Treated i.o. lesions (70–90 days post-PDT) were free of tumor cells and demonstrated fibrosis and new bone formation in the medullar cavity, whereas the bone cortex was mainly necrotic (Fig. 5*a*). A complete curative response, defined by both free movement of the animal, the absence of visible tumors and tumor-free histopathology (>70 days post-PDT), was observed in 11/22 (50%) of the treated mice. In contrast, the dark/light control tumors at 50 days post-treatment revealed an abundance of viable tumor cells in the medullar cavity, with cells infiltrating the bone cortex periosteum and the surrounding tissue (Fig. 5*b*). PDT on a healthy mouse leg exhibited a slight but transient inflammation on the skin and muscle but no necrosis or injury to the bone (data not shown).

The orthotopic model of WISH PC2

Since these experiments were conducted on human PC within the murine host, we next examined the effect of this novel PDT protocol by modeling interstitial illumination on the tumor within its inherent anatomical location in the prostate microenvironment. The total light dose used with the diffuser equipped fiber was 54 J/0.6 cm (30 mW/0.6 cm/30 min), since preliminary experiments to define the appropriate illumination parameters showed that higher light doses led to injury of the neighboring tissues (data not shown). Histopathological examination of the tumor 24 hr after PDT showed diffuse coagulation necrosis of >95% of the tumor (Fig. 5*c*). Some sparing of viable cells (~ 5%) was limited to the periphery and occasionally admixed with extravasated red blood cells. At 48 hr post-PDT (Fig. 5*d*), similar histological changes were seen, but the hemorrhages were more widely spread. In agreement with the results described above, the plasma hCgA levels dropped by 80–90% by 48 hr after PDT.

DISCUSSION

We described the application of TOOKAD-based PDT on a localized human prostate cancer xenograft model and its bone metastases. The success of this treatment protocol is based on the photochemical properties of the sensitizer (*i.e.*, an absorption band at 750–775 nm with a high extinction coefficient) and its damage to the tumor vasculature. Local control of either primary PC or symptomatic discrete PC metastases (*e.g.*, symptomatic bone lesions and tumor mass effects of metastatic lymph nodes) may now be feasible with TOOKAD-PDT, offering successful eradication of bulky PC tumors. This was so far not achieved in the clinic in the case of human PC with PDT protocols based on sensitizers like Photofrin or aminolevolinic acid (ALA). The limited depth of light penetration that restricted tumor response to a few millimeters and the prolonged skin phototoxicity of these sensitizers deem the respective PDT protocols inapplicable for treatment of PC.[41,42]

Indeed, the enhanced light penetration in the case of TOOKAD-PDT-induced necrosis to a depth of 1.3 cm in bulky WISH-PC2 tumors (Fig. 2*a*) and a substantial curative effect of the intraosseous tumor lesions upon transcutaneous illumination (Figs. 3*a*, 4*a–c*, 5*a*). The sensitizing light penetration and interstitial distribution have become major factors in predicting success in the PDT of solid tumors within visceral organs such as the human prostate ranging in volume from 30–50 ml. This notion is further supported by the ability of the suggested TOOKAD-PDT protocol to specifically destroy prostatic tissue with minimal side effects.[23] It is therefore expected that TOOKAD-PDT of human PC should be advantageous over other sensitizers that have longer clearance rates[25] and absorb at shorter wavelengths previously examined by others for prostate tissue-transparency in experimental animals.[17,19] Although the depth of PDT-induced necrosis is greater than the illumination depth, interstitial laser light delivery may include multiple fibers to enable the effective treatment of substantial masses of the prostate.[36] Indeed, tumors within the prostate are amenable to interstitial illumination that can be applied transrectally or transperineally under the guidance of real time transrectal ultrasonography. Since the prostate is not a vital organ, normal tissue damage is acceptable and even desirable (in total PC ablation) since it may reduce local recurrence. Application of TOOKAD-PDT in a normal canine prostate model was reported to induce necrotic lesions of over 3 cm in diameter, while the animals recovered well without urethral complications.[23] There was no structural or functional urethral damage even when the urethra was within the treated region. Moreover, the light scattered from the prostate did not cause damage to the nearby rectum or bladder, suggesting that their normal structure can be safely preserved on the basis of optimal dosimetry. These results therefore suggest that TOOKAD-PDT may be a promising modality for future treatment prostate cancer.[23]

In using TOOKAD-PDT on well-defined s.c. tumors in order to model localized PC, a single treatment session successfully eradicated the tumors, yielding a cure rate of 69% or even slightly higher, 77% (considering the death of 3 mice from an undetermined cause) (Fig. 1*a*,*d*). The response of the prostatic tumor mass

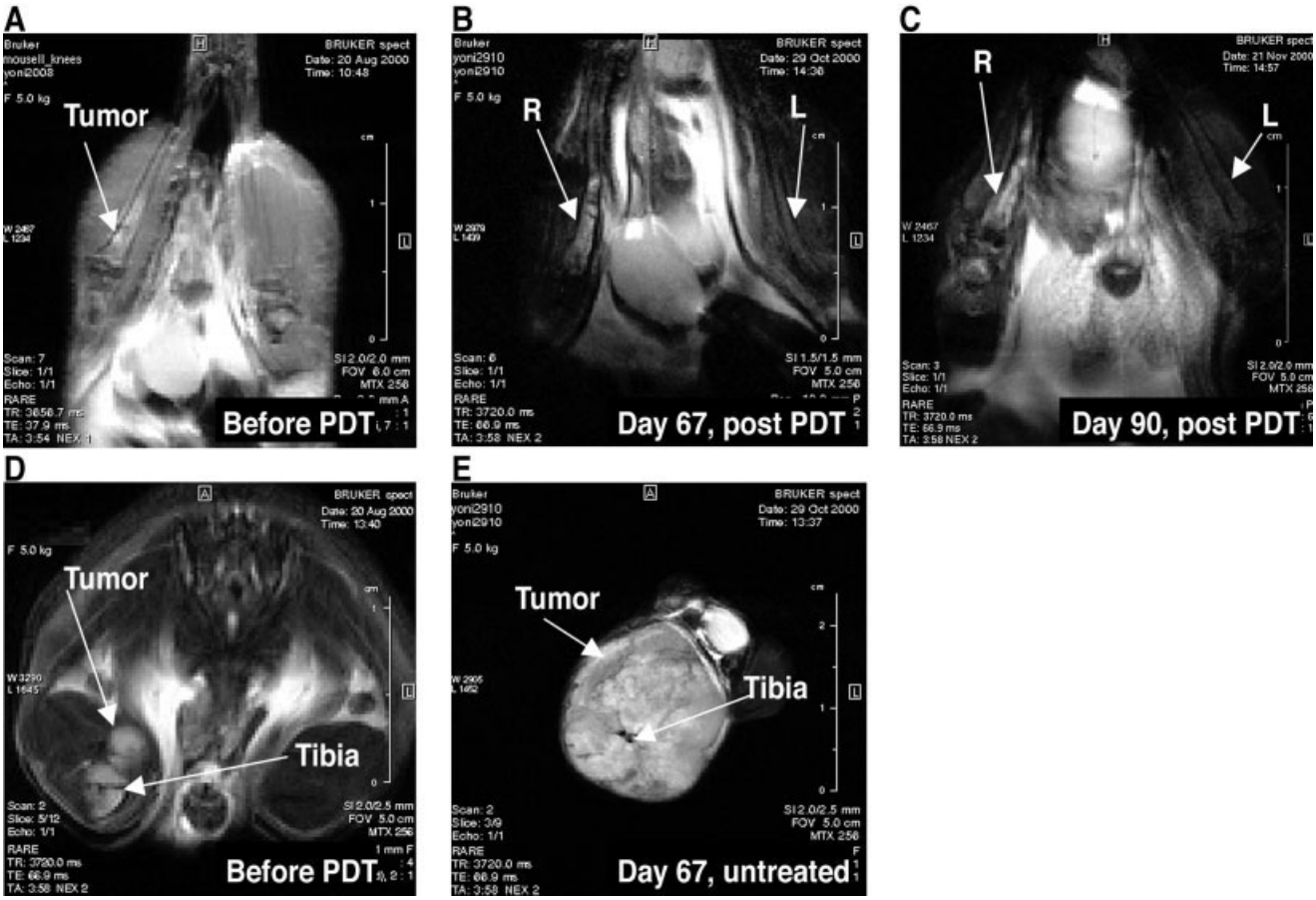

FIGURE 4 – TOOKAD-based PDT of human WISH-PC2 bone lesion model: MRI evaluation. Tumor location within the tibia was determined by MRI, as described in Material and Methods. Coronal (*a*) and axial (*d*) sections of intratibial WISH-PC2 implants are shown before PDT. Following PDT, high intensity material can be seen at the treatment site at 67 days (*b*) and 90 days (*c*), histologically shown in Figure 5*a*, whereas untreated tumor (Axial section) (*e*) continued to grow.

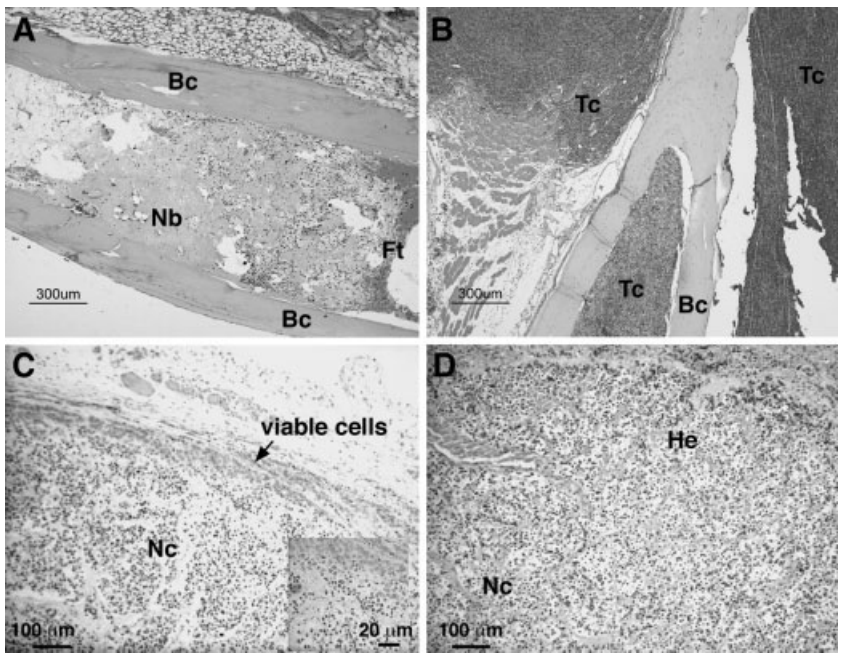

FIGURE 5 – TOOKAD-based PDT of human WISH-PC2 intraosseous and orthotopic grafts: histopathological evaluation. (*a*) PDT-treated bone at 90 days after treatment. No tumor cells are seen in the medullar cavity and in the surrounding tissue. There is fibroplasia (Ft) and a deposition of disorganized woven new bone (Nb) within the medullar cavity. The bone cortex (Bc) is mostly necrotic. (*b*) In the dark control there is uncontrolled growth of tumor cells (Tc) filling the medullar cavity and forming large tumor masses in the surroundings. The intact bone cortex contains viable osteoblasts. (*c*) In the orthotopic tumor model at 24 hr after PDT, necrotic (Nc) and isolated peripheral groups of viable cells (Vc) were observed. (*d*) At 48 hr post-PDT, extensive necrosis with multifocal hemorrhages developed.

in the orthotopic model, as monitored histologically, also verified the concept in the prostatic microenvironment (Fig. 5*c*,*d*). We obtained similar cure rates with TOOKAD-PDT in treatment of other solid tumors like C6 rat glioma (64 %)[33] and with PDT using Bacteriochlorophyll-Serine (the predecessor of TOOKAD) in the cases of mouse melanoma (80 %)[31] and rat DS sarcoma (80 %).[32]

The recurrence or post-treatment dissemination of PC can be detected at early stages by monitoring prostate specific antigen (PSA) levels, a serum tumor marker of PC.[39] In our study, we took advantage of the inherited surrogate marker hCgA of the WISH PC2 model to monitor the treatment response to PDT37. A highly significant increase of plasma hCgA levels accompanied tumor growth in the control animals, whereas hCgA levels in PDT-treated animals declined and became practically undetectable (Fig. 1).

As shown in this work, the necrotic process (24–48 hr) was initiated by vascular damage, hemorrhage and blood stasis (1–48 hr), leading to the complete destruction of the tumor with consequent tissue remodeling 10 days after PDT (Fig. 2). Moreover, the effects on the surrounding normal tissue were mild and transient, presumably due to the greater fragility of the tumor neovasculature and the relative resistance of the normal vasculature. Previously, it was shown that vascular damage and the subsequent tumor cell anoxia are indirect mechanisms that lead to tumor necrosis.[43,44] PDT with Photofrin in mice led to macromolecular leakage from blood vessels and to vascular constriction during the illumination.[45] In PDT with Bacteriochlorophyll-Serine, vascular insult, macromolecular leakage and blood stasis seem to play a primary role in tumor destruction, as previously shown in our laboratory.[31]

Generation of ROS by photosensitization is a hallmark of PDT[2-4] with one of the recorded cell/tissue responses being LPO.[46,47] Lipid peroxidation leads to cell injury and death[48] and has been implicated in the pathogenesis of oxidative stress of numerous diseases.[49,50] It was therefore interesting to test if PDT-induced oxidative stress could be traced by positive staining for peroxide products in treated tumor sections. Peroxides of polyunsaturated ω-6 fatty acids are converted into aldehydes like HNE, which are highly reactive by themselves and considered secondary toxic messengers that disseminate and augment initial free radical events.[49,51] HNE can also spontaneously conjugate to proteins and be immunohistologically traced with anti-HNE antibodies and serve as an LPO marker.[40]

Untreated tumors that contained intact viable tumor cells stained negative for HNE (Fig. 2*k*). In contrast the development of necrosis in the tumor was preceded by intense LPO, detected 1hr after PDT in the form of HNE staining within in the boundary of the tumor blood vessels but not in surrounding tumor cells (Fig. 2*l*). Further spreading of HNE staining in the tumor mass continued at later times (16–48 hr, Fig. 2*m–o*). Within this temporal and spatial process, one can identify 2 distinct phases: (i) selective blood vessel associated HNE staining observed at <1 hr after illumination that can be identified with the primary photogeneration of ROS (Fig. 2*l*) and (ii) secondary light-independent HNE-facilitated peroxide generation of radicals associated with ischemia that culminates in complete necrosis and tissue disintegration within <10 days after treatment (Fig. 2*m–o*). The relative contribution of the primary and secondary phases of LPO production to the overall therapeutic effect of TOOKAD-PDT has yet to be explored. Interestingly, normal tissue sparing could be verified histologically by this method, demonstrating negative HNE staining of connective tissue within the tumor (Fig. 2*o*).

Thus, our study suggests that photosensitization of TOOKAD is primarily confined to the tumor blood vessels with consequential functional damage and stasis as recently reported by us in melanoma tumors.[52] However, massive tumor damage and necrosis develop subsequent to treatment as a result of a secondary wave of oxidative damage marked by LPO that spreads to cover the entire tumor. Furthermore, TOOKAD-PDT is more confined to the neoplastic component of the tumor for reasons that are presently unclear. Preservation of subepithelial mature collagen following Photofrin-PDT has been previously reported.[53]

Prostatic small cell carcinoma is an aggressive malignancy with a very poor prognosis. One of the typical clinical features of SCCP is its tendency to develop visceral metastasis. The most frequent metastatic sites of SCCP are the bones (55%), regional and distant lymph nodes (52%), and the liver (48%).[54] No effective treatment for systemic SCCP has been established, most probably because of the limited patient population and the aggressiveness of the disease.[55] To model bone metastases, we applied transcutaneous PDT with TOOKAD for bone lesions of WISH-PC2 (Figs. 3–5*a*,*b*), obtaining a 50% long-term cure rate. Although bone lesions invariably appear in the context of disseminated disease, they manifest clinically with unique morbidity and sequel. Consequently, we suggest that isolated bone lesions that, for example, endanger weight bearing areas or the integrity of the spinal cord could be clinically addressed by this accurate local treatment modality that offers treatment to larger tumors than was formally possible with PDT. It is anticipated that direct interstitial fiber optic light delivery will be used for optimal clinical results including intraosseus treatment. To the best of our knowledge, this is the first reported experimental treatment of tumor bone lesions by PDT, most likely enabled by the near infrared absorption of the TOOKAD.

In summary, currently concentrating on the most violent type of PC, we have demonstrated that TOOKAD-PDT may offer a promising treatment option for primary prostate cancer or problematic prostate cancer metastasis (*e.g.*, bone lesions). Future studies will address the response of human prostatic adenocarcinoma xenografts by applying the knowledge gained in our study.

ACKNOWLEDGEMNTS

Y.S. is the incumbent of the Tillie and Charles Lubin Professorial Chair in Biochemical Endocrinology. A.S. is the incumbent of the Robert and Yadele Sklare Professional Chair in Biochemistry. The authors thank Professor E. Schechtman for her advice in the statistical analyses, Dr. P. Harve Brun for helpful discussions, R. Tsoref for her excellent secretarial help and Ms. R. Garner for help in English editing.

REFERENCES

1. Henderson BW, Dougherty TJ. How does photodynamic therapy work? Photochem Photobiol 1992;55:145–57.
2. Kato H, Patrice T, Wilson B. Photodynamic therapy. In: Johnson S, Johnson FN, eds. Review of Contemporary Pharmacotherapy. London: Marius Press, 1999. 1–78.
3. Dougherty TJ, Gomer CJ, Henderson BW, Jori G, Kessel D, Korbelik M, Moan J, Peng Q. Photodynamic therapy. J Natl Cancer Inst 1998;90:889–905.
4. Macdonald IJ, Dougherty TJ. Basic principles of photodynamic therapy. J Porphyrins Phthalocyanines 2001;5:105–29.
5. Peng Q, Soler AM, Warloe T, Nesland JM, Gierckskey K. Selective distribution of porphyrins in skin thick basal cell carcinoma after topical application of methyl 5-aminolevulinate. J Photochem Photobiol B 2001;62:140–5.
6. Kubler AC, Haase T, Staff C, Kahle B, Rheinwald M, Muhling J. Photodynamic therapy of primary nonmelanomatous skin tumours of the head and neck. Lasers Surg Med 1999;25:60–8.
7. Maier A, Tomaselli F, Matzi V, Rehak P, Pinter H, Smolle-Juttner FM. Photosensitization with hematoporphyrin derivative compared to 5-aminolaevulinic acid for photodynamic therapy of esophageal carcinoma. Ann Thorac Surg 2001;72:1136–40.
8. Ost D. Photodynamic therapy in lung cancer. Oncology (Huntington) 2000;14:379–86, 91; discussion 91–2, 95.
9. Moghissi K, Dixon K, Stringer M, Freeman T, Thorpe A, Brown S. The place of bronchoscopic photodynamic therapy in advanced unresectable lung cancer: experience of 100 cases. Eur J Cardiothorac Surg 1999;15:1–6.
10. D'Hallewin MA, Baert L. Long-term results of whole bladder wall

photodynamic therapy for carcinoma in situ of the bladder. Urology 1995;45:763–7.
11. Zupko I, Kamuhabwa AR, D'Hallewin MA, Baert L, De Witte PA. In vivo photodynamic activity of hypericin in transitional cell carcinoma bladder tumors. Int J Oncol 2001;18:1099–105.
12. Nseyo UO. Photodynamic therapy in the management of bladder cancer. J Clin Laser Med Surg 1996;14:271–80.
13. Nseyo UO, DeHaven J, Dougherty TJ, Potter WR, Merrill DL, Lundahl SL, Lamm DL. Photodynamic therapy (PDT) in the treatment of patients with resistant superficial bladder cancer: a long-term experience. J Clin Laser Med Surg 1998;16:61–8.
14. Pantelides ML, Whitehurst C, Moore JV, King TA, Blacklock NJ. Photodynamic therapy for localised prostatic cancer: light penetration in the human prostate gland. J Urol 1990;143:398–401.
15. Whitehurst C, Pantelides ML, Moore JV, Blacklock NJ. Optimization of multifiber light delivery for the photodynamic therapy of localized prostate cancer. Photochem Photobiol 1993;58:589–93.
16. Whitehurst C, Pantelides ML, Moore JV, Brooman PJ, Blacklock NJ. In vivo laser light distribution in human prostatic carcinoma. J Urol 1994;151:1411–5.
17. Lee LK, Whitehurst C, Pantelides ML, Moore JV. In situ comparison of 665 nm and 633 nm wavelength light penetration in the human prostate gland. Photochem Photobiol 1995;62:882–6.
18. Chen Q, Hetzel F. Laser dosimetry studies in the prostate. J Clin Laser Med Surg 1998;16:9–12.
19. Arnfield MR, Chapman JD, Tulip J, Fenning MC, McPhee MS. Optical properties of experimental prostate tumors in vivo. Photochem Photobiol 1993;57:306–11.
20. Chang SC, Buonaccorsi GA, MacRobert AJ, Bown SG. Interstitial photodynamic therapy in the canine prostate with disulfonated aluminum phthalocyanine and 5-aminolevulinic acid-induced protoporphyrin IX. Prostate 1997;32:89–98.
21. Momma T, Hamblin MR, Wu HC, Hasan T. Photodynamic therapy of orthotopic prostate cancer with benzoporphyrin derivative: local control and distant metastasis. Cancer Res 1998;58:5425–31.
22. Moore RB, Chapman JD, Mercer JR, Mannan RH, Wiebe LI, McEwan AJ, McPhee MS. Measurement of PDT-induced hypoxia in Dunning prostate tumors by iodine-123-iodoazomycin arabinoside. J Nucl Med 1993;34:405–11.
23. Chen Q, Huang Z, Luck D, Beckers J, Brun PH, Wilson BS, Scherz A, Salomon Y, Hetzel FW. Preclinical studies in normal canine prostate of a novel Palladium-Bacteriopheophorbide (WST09) photosensitizer for photodynamic therapy of prostate cancer. Photochem Photobiol 2002;76:438–45.
24. Windahl T, Andersson SO, Lofgren L. Photodynamic therapy of localised prostatic cancer. Lancet 1990;336:1139.
25. Kessel D, Dougherty T. Agents used in photodynamic therapy. In: Johnson S, Johnson FN, eds. Review of Contemporary Pharmacotherapy London: Marius Press, 1999. 19–24.
26. Scherz A, Feodor L, Salomon Y. Chlorophyll and bacteriochlorophyll derivatives, their preparation and pharmacological compositions comprising them. Patent Application No. 5,650,292. USA, 1997.
27. Scherz A, Fiedor L, Salomon Y. Chlorophyll and bacteriochlorophyll derivatives, their preparation and pharmaceutical compositions comprising them. II. Patent Application No. 5,726,169. USA, 1998.
28. Scherz A, Salomon Y, Scheer H, Brandis A. Palladium-substituted bacteriochlorophyll derivatives and use thereof. International PCT Patent Application No. PCT/IL99/00673, 1999.
29. Rosenbach-Belkin V, Chen L, Fiedor L, Tregub I, Paviotsky F, Brumfeld V, Salomon Y, Scherz A. Serine conjugates of chlorophyll and bacteriochlorophyll: photocytotoxicity in vitro and tissue distribution in mice bearing melanoma tumors. Photochem Photobiol 1996; 64:174–81.
30. Rosenbah-Belkin V, Chen L, Fiedor L, Tregub I, Pavlotsky F, Brumfeld V, Salomon Y, A.Scherz. Chlorophyll and bacteriochlorophyll derivatives as photodynamic agents. In: Moser J, ed. Photodynamic tumor therapy: 2nd and 3rd generation photosensitizers. London: Harwood Academic Publishers, 1998. 117–26.
31. Zilberstein J, Schreiber S, Bloemers MC, Bendel P, Neeman M, Schechtman E, Kohen F, Scherz A, Salomon Y. Antivascular treatment of solid melanoma tumors with bacteriochlorophyll-serine-based photodynamic therapy. Photochem Photobiol 2001;73:257–66.
32. Kelleher DK, Thews O, Rzeznik J, Scherz A, Salomon Y, Vaupel P. Water-filtered infrared-A radiation: a novel technique for localized hyperthermia in combination with bacteriochlorophyll-based photodynamic therapy. Int J Hyperthermia 1999;15:467–74.
33. Schreiber S, Gross S, Brandis A, Harmelin A, Rosenbach-Belkin V, Scherz A, Salomon Y. Local photodynamic therapy (PDT) of rat C6 glioma xenografts with Pd-Bacteriopheophorbide leads to decreased metastases and increased animal cure compared to surgery. Int J Cancer 2001;99:279–85.
34. Mazor O, Brandis A, Gross S, Hami R, Vakrat Y, Koudinova N, Gladysh E, Kostenitz G, Orenstien A, Salomon Y, Scherz A. Pd-Bacteriopheophorbide (TOOKAD), a novel anti-vascular agent for photodynamic therapy of tumors: in vitro and in vivo studies. FISEB Eilat, Israel, 2002. Abstract book:231.
35. Schreiber S, Gross S, Harmelin A, Brandis A, Salomon Y, Sherz A. Photodynamic therapy (PDT) of rat C6 glioma xenografts with Pd-Pheophorbide (TOOKAD) leads to decreased metastases and increased animal cure compared to surgery. IPA 8th International Congress of Photodynamic Medicine. Vancouver, Canada, 2001.
36. Lee LK, Whitehurst C, Pantelides ML, Moore JV. An interstitial light assembly for photodynamic therapy in prostatic carcinoma. BJU Int 1999;84:821–6.
37. Pinthus JH, Waks T, Schindler DG, Harmelin A, Said JW, Belldegrun A, Ramon J, Eshhar Z. WISH-PC2: a unique xenograft model of human prostatic small cell carcinoma. Cancer Res 2000;60:6563–7.
38. Rembrink K, Romijn JC, van der Kwast TH, Rubben H, Schroder FH. Orthotopic implantation of human prostate cancer cell lines: a clinically relevant animal model for metastatic prostate cancer. Prostate 1997;31:168–74.
39. Gleave ME, Hsieh JT, Wu HC, von Eschenbach AC, Chung LW. Serum prostate specific antigen levels in mice bearing human prostate LNCaP tumors are determined by tumor volume and endocrine and growth factors. Cancer Res 1992;52:1598–605.
40. Uchida K, Itakura K, Kawakishi S, Hiai H, Toyokuni S, Stadtman ER. Characterization of epitopes recognized by 4-hydroxy-2-nonenal specific antibodies. Arch Biochem Biophys 1995;324:241–8.
41. Wan S, Parrish JA, Anderson RR, Madden M. Transmittance of non-ionising radiation in human tissue. Photochem Photobiol 1981; 34:679–81.
42. Bonnett R. Photodynamic therapy in historical perspective. In: Johnson S, Johnson FN, eds. Reviews in contemporary pharmacotherapy. London: Marius Press, 1999. 1–14.
43. Fingar VH, Wieman TJ, Wiehle SA, Cerrito PB. The role of microvascular damage in photodynamic therapy: the effect of treatment on vessel constriction, permeability, and leukocyte adhesion. Cancer Res 1992;52:4914–21.
44. Fingar VH. Vascular effects of photodynamic therapy. J Clin Laser Med Surg 1996;14:323–8.
45. Fingar VH, Wieman TJ, Haydon PS. The effects of thrombocytopenia on vessel stasis and macromolecular leakage after photodynamic therapy using photofrin. Photochem Photobiol 1997;66:513–7.
46. Chatterjee SR, Srivastava TS, Kamat JP, Devasagayam TP. Lipid peroxidation induced by a novel porphyrin plus light in isolated mitochondria: possible implications in photodynamic therapy. Mol Cell Biochem 1997;166:25–33.
47. Hadjur C, Richard MJ, Parat MO, Jardon P, Favier A. Photodynamic effects of hypercin on lipid peroxidation and antioxidant status in melanoma. Photochem Photobiol 1996;64:375–81.
48. Pradhan D, Weiser M, Lumley-Sapanski K, Frazier D, Kemper S, Williamson P, Schlegel RA. Peroxidation-induced perturbations of erythrocyte lipid organization. Biochim Biophys Acta 1990;1023: 398–404.
49. Esterbauer H, Schaur RJ, Zollner H. Chemistry and biochemistry of 4-hydroxynoneal, malonaldehyde and related aldehydes. Free Radic Biol Med 1991;11:81–128.
50. Halliwell B, Gutteridge JM. Free radicals in biology and medicine. Oxford: Oxford University Press, 1999.
51. Uchida K, Shiraishi M, Naito Y, Torii Y, Nakamura Y, Osawa T. Activation of stress signaling pathways by the end product of lipid peroxidation: 4-hydroxy-2-nonenal is a potential inducer of intracellular peroxide production. J Biol Chem 1999;274:2234–42.
52. Gross S, Gilead A, Scherz A, Neeman M, Salomon Y. Photodynamic therapy (PDT) of solid tumors with Pd-Bacteriopheophorbide (WST09): functional imaging by blood oxygen level-dependent (BOLD) MRI. 10th International Society for Magnetic Resonance in Medicine. Honolulu, Hawaii, 2002. Abstract 2154.
53. Grant WE, Speight PM, Hopper C, Bown SG. Photodynamic therapy: an effective, but non-selective treatment for superficial cancers of the oral cavity. Int J Cancer 1997;71:937–42.
54. Abbas F, Civantos F, Benedetto P, Soloway MS. Small cell carcinoma of the bladder and prostate. Urology 1995;46:617–30.
55. Amato RJ, Logothetis CJ, Hallinan R, Ro JY, Sella A, Dexeus FH. Chemotherapy for small cell carcinoma of prostatic origin. J Urol 1992;147:935–7.